Scientific Review Engineering and Environmental Sciences (2023), 32 (1), 69–86

Sci. Rev. Eng. Env. Sci. (2023), 32 (1) https://srees.sggw.edu.pl

ISSN 1732-9353 (suspended) eISSN 2543-7496 DOI 10.22630/srees.4506

Received: 11.10.2022
Accepted: 30.01.2023

Layth Abdul Rasool ALASADI✉ https://orcid.org/0000-0001-6244-7965
Tagreed Hameed KHLIF https://orcid.org/0000-0002-0429-796X
Fadhel Abdulabbas HASSAN https://orcid.org/0000-0003-1020-5133
University of Kufa, Faculty of Engineering, Department of Structures and Water Resources, Iraq

Experimental investigation for the local scour around V-shaped spur-dikes

Keywords: local scour, clearwater conditions, V-shaped spur-dyke, checkmark spur-dyke, river training structure, sediment transport

Introduction

Rivers are considered one of the greatest reasons for the existence of human being gathering. They convey and collect downfall as natural flows, and hence rivers are supposed to be the main source of water that must be mastered, restrained, and controlled to meet the requirements of human beings. In general, humans shape their existence alongside the rivers, where these situations have many advantages and disadvantages. One of the disadvantages is the destruction by river floodings and erosion of their banks, so rivers should be controlled in order to minimize their severity. Also, one should know any critical points of rivers and use biological or mechanical ways to reduce erosion, such as river training structures (Espandar & Imam, 1994; Rashad & Kassaf, 2020). The most common and beneficial transversal river training structures are spur-dikes (Al-Yassiry, 2015), i.e. artificial networks situated on river banks at various angles with one edge on the bank and the other edge outstanding into the current. Spur-dikes are constructed and created

✉laitha.alasadi@uokufa.edu.iq

Alasadi, L. A. R., Khlif, T. H., Hassan, F. A. (2023). Experimental investigation for the local scour around V-shaped spur-dikes. *Sci. Rev. Eng. Env. Sci.*, *32* (1), 69–86. DOI 10.22630/srees.4506

for many purposes, such as: directing the flow for the chosen reach, increasing the flow depth for navigation, preventing erosion of rivers banks, establishing river alignment and cross-section, enhancing habitats of riverine aquatic, altering the surrounding view and aiding the accessibility to the river (Jafari & Masjedi, 2015; Rashad, 2021). Spur-dikes are typically made from stone, gravel, rock, earth, sand, or piles. They can be either submerged or non-submerged. The non-submerged ones are made in the case of impermeable spur-dikes since their top is exposed to severe erosion if submerged. On the other hand, spur-dikes can be designed in different plan view shapes, such as I, L, T, hockey, inverted hockey, and curved shapes (Fig. 1).

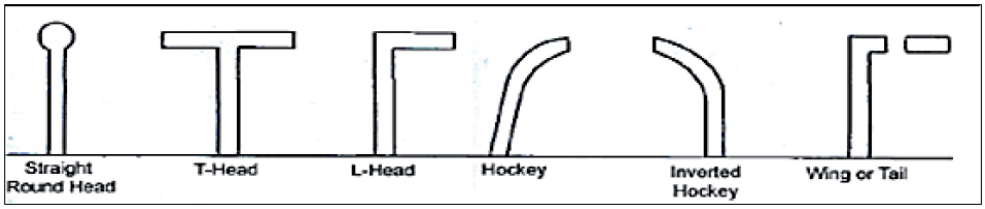

FIGURE 1. Different shapes of spur-dikes
Source: own work.

Against all spur-dike advantages and like any obstruction or hydraulic structure in an alluvial river, the natural river balance will be disturbed when a spur-dike crosses the water. So, as a result, a significant disruption in the flow pattern around the structure foundation will take place. This disruption leads to the scouring process initiation that ends with spur-dikes instability and time, which then leads to the failure in spur-dikes foundations. For hydraulic engineers, the local scour around spur-dykes is essential in the design process to ensure safety and economic purposes. Over the years, numerous researchers studied the most efficient factors affecting the scour process and the maximum exploration depth (Khsaf, 1991). His experimental study on a series of impermeable spur-dikes took place in the laboratory flume; it stated that the higher the scouring depth, the bigger the Froude number, degree of inclination angle and opening ratio. Kurzke, Weitbrecht and Jirka (2002) proved that spur-dike fields mainly generate two eddies; the larger one is in the spur-dike field center and the other in the upper corner of the spur-dike area. Kadota and Suzuki (2010) studied the effect of changing the shape of spur-dikes (L- and T-shapes) on the characters and trends of local scour around them. Through experiments, they proved that the T-shape spur-dikes had smaller local scour in the downstream area and, to some extent, from the spur-dike; a deposition takes place. Al-Yassiry (2015) tested non-traditional shapes of spur-dikes, which are the curved ones, and proved

that these shapes could minimize the local scour to some extent and gave better performance than the traditional shapes. Al Shaikhli and Kadhim (2018) studied the local scour around impermeable spur-dikes, submerged, single and straight in shape, fixed in a non-curved laboratory flume, and have various angle inclinations regarding flow direction. They proved that the horseshoe vortices are the leading cause of scour around spur-dike. The goals of the present study are to use the specific shape of spur-dikes that have the advantages of simple and low cost in construction, manageable scour at spur-dikes heads, large sediment deposits inside spur-dikes fields, and reasonable protection of the banks of rivers. This shape is the checkmark shape, also referred to as the V-shape. Also, this study presents two effective countermeasures for minimizing local scour around this kind of spur-dikes. These countermeasures are spur-dike numbers and the space between them.

Mechanisms of local scour

The scour is mainly defined as a naturalist event resulting from the flowing water's erosive behavior upon the banks and beds of alluvial channels. Scour is also defined as the sediment sweeping near or around structures placed inside the flowing water. So a reduction in the river bed level came from water erosions, which will have a tendency to reveal the structure foundations or carve and transport materials of the banks and bed of streams away from their original locations (Ezzeldin, Saafan, Rageh & Nejm, 2007). Such a phenomenon around any obstructions will progress continuously, leading to undermining and failure in the obstruction's foundations, collapsing all the hindrances and loss of life, nearby lands and properties. As regards the mechanism of the local scour, it should be stated that the existence of a spur-dike structure in the watercourse will cause contraction at the site and hence trigger vortices of the complicated system at the spur-dikes root, which is considered to be the main reason for scouring along with downflow at the spur-dike upstream face (Toro-Escobar, Voigt, Melville, Chiew & Parker, 1998; Fig. 2).

Figure 2 also displays how the horseshoe shaped vortex bumps the sand bed immediately ahead of the spur-dike and then holds up the corroded sediments, which will be transported in the direction of the flow by the main flow itself. There are four

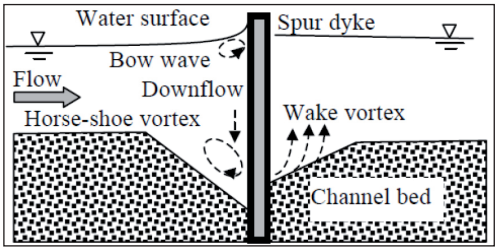

FIGURE 2. Local scour and flow through the section that passes the spur-dike head

Source: Toro-Escobar et al. (1998).

Alasadi, L. A. R., Khlif, T. H., Hassan, F. A. (2023). Experimental investigation for the local scour around V-shaped spur-dikes. *Sci. Rev. Eng. Env. Sci.*, *32* (1), 69–86. DOI 10.22630/srees.4506

serial stages of the scour hole development before reaching their final shape: initiation stage, development stage, stabilization stage, and equilibrium stage. It should be mentioned that the flow conditions control the shifting from one stage to another through time. In explicit water situations where the flow velocity is less than critical velocity, rapid development occurs for scouring until the dimensions of scour holes are no longer expanding and the maximum scouring depth is reached. In the case of live bed scour conditions where the flow velocity is more significant than the critical velocity and flow transports, in general, the bed and sides material. A quick reaching for the depth of scour holes oscillates with time due to the entrance and exit of the eroded sediments from the scour holes (Lagasse & Richardson, 2001; Fig. 3).

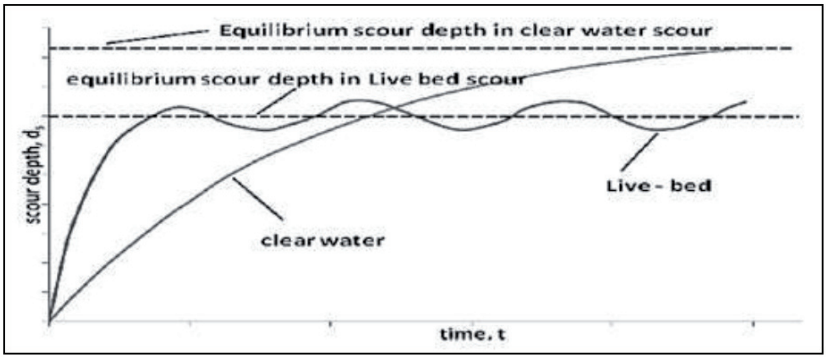

FIGURE 3. Clear-water and live-bed scour conditions
Source: Lagasse and Richardson (2001).

Various methods, like empirical formulas, physical models and theoretical approaches, are used to study and determine the scour depths around spur-dikes. In the present study, a group of physical models was used in a series of experiments. Then the results were used to shape an empirical formula to predict the maximum local scour under specific conditions.

Dimensional analysis

This technique is mathematical and employed in research studies to perform and design experiment models. Using this technique for a V-shaped spur-dike, the maximum depth of the local scour ($d_{s\max}$) at the clear water state located in this spur-dike nose can be inscribed as:

$$d_{s\max} = f\{y, v, v_c, L_g, \rho, \rho_s, g, n, b, d_{50}, \mu, \sigma_g, B, S_\circ\}, \quad (1)$$

where: y – depth of discharge [-], v – speed of the main flow [m·s^{-1}], v_c – critical velocity [m·s^{-1}], L_g – spur-dikes length [m], ρ – fluid density [kg·m^{-3}], ρ_s – bed sediments density [kg·m^{-3}], g – gravitational acceleration, g = 9.80665 [m·s^{-2}], n – number of spur-dikes, b – distance between spur-dikes [mm], d_{50} – median particle size [-], μ – fluid dynamic viscosity [Pa·s], σ_g – geometric standard deviation [-], B – laboratory flume width [m], $S_\circ$ – flume slope [m/m],

By using the Buckingham's π theorem; and after several arrangements and simplifications, Eq. (1) becomes:

$$d_{s\max}/y = f(v/v_c, F_r, n, b/y). \tag{2}$$

The assumptions and principles of transforming Eq. (1) simplified Eq. (2) are explained and described in more detail in the appendix.

The laboratory flume

Figure 4 shows the laboratory flume utilized in this study. It was made of steel stiffeners for the mainframe and glass fiber for the sides, with a total length of 6.6 m and an inner cross-section of 0.4 × 0.4 m. Two flume consists of two

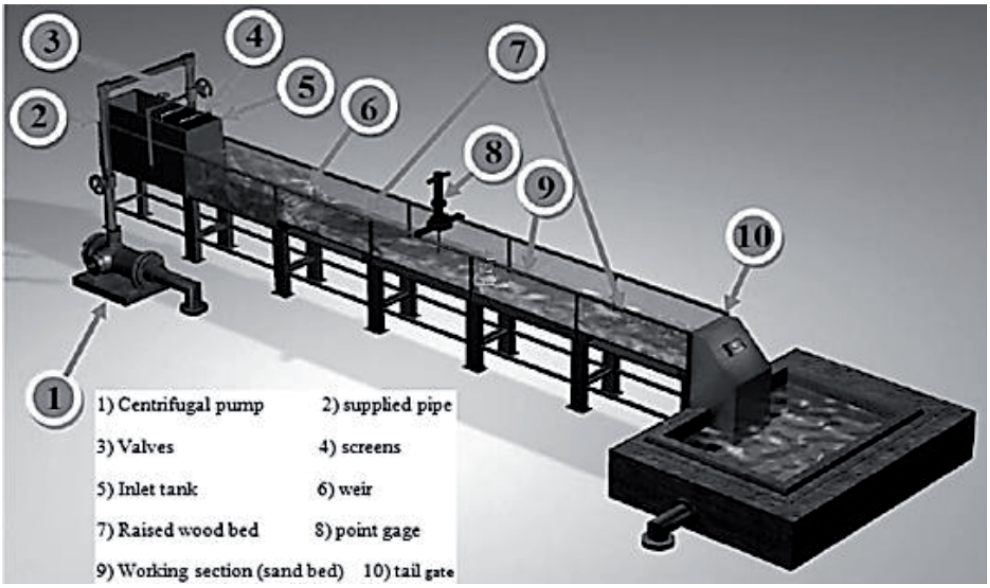

FIGURE 4. The laboratory flume
Source: own work.

Alasadi, L. A. R., Khlif, T. H., Hassan, F. A. (2023). Experimental investigation for the local scour around V-shaped spur-dikes. *Sci. Rev. Eng. Env. Sci.*, *32* (1), 69–86. DOI 10.22630/srees.4506

essential parts; an upstream inlet tank has a 1 m height and the second is a 5.6 m working section.

The middle part of the working section was covered with 0.1 m deep and 2 m long erodible sediments. The other two parts of the operating section were covered with wooden plates to match the level of the middle part. The inlet tank has three screens to prevent contamination with any undesirable debris. The flume had a closed system for supplying water from an underground basin using a centrifugal pump next to the flume. At the end of the flume, an adjustable tailgate was used to control the flow depth in the working section. A fabricated sharp-crested rectangular weir, 0.4 m wide and 0.25 m high, was placed at the upstream flume section to measure the entering discharge to the working section. The weir covered the full rectangular flume width and was made from Plexiglas® fiber. All scour depth measurements are done with a movable point gauge with ±1 mm accuracy transversely and longitudinally above the operating section.

The water discharges applied in this study were obtained by measuring the weir head over it; then, using the weir function – equation (King, Brater, Wei & Lindell, 1996):

$$Q = C_e \, L_e H^{\frac{3}{2}}, \tag{3}$$

where: Q – weir discharge [$m^3 \cdot s^{-1}$], C_e – effective discharge coefficient, $C_e = 1.78 + 0.24^{\frac{H}{P}}$ [-], H – head over weir crest measured before weir by 0.1 m [m], P – weir height from the bed [m], L_e – effective length, $L_e = L + K_L$, in which: L is a length of the weir, and K_L is a length factor, set to 0 [m], H_e – effective head over the weir, $H_e = H + K_H$, in which: K_H – head factor, set to 0.001 [-].

Spur-dike models

This study used a checkmark or V-shaped spur-dikes, 10-milimeter thick, 12-centimeter net high and 13-centimeter long, perpendicular to the flow direction where the length should be not less than 1/3 of the width of the flume (Möws & Koll, 2019; Fig. 5). The models were made of non-swelling polystyrene foam material. They have conducted

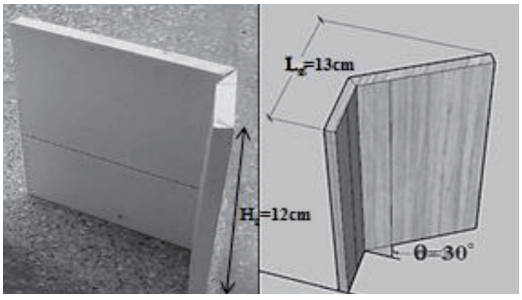

FIGURE 5. The V-shaped spur-dike model
Source: own work.

experiments under three different arrangements (triple, double and single). Also, the distance between them was altered three times ($1L_g$, $1.5L_g$, $2L_g$).

To achieve an adequately established flow, the models were positioned straight up through the sediment stratum in the working section center, where silicon adhesive was used to glue the spur-dikes very well to the inner side of the flume. Figure 6 illustrates a V-shaped spur-dike fixed in its place before beginning the experiments.

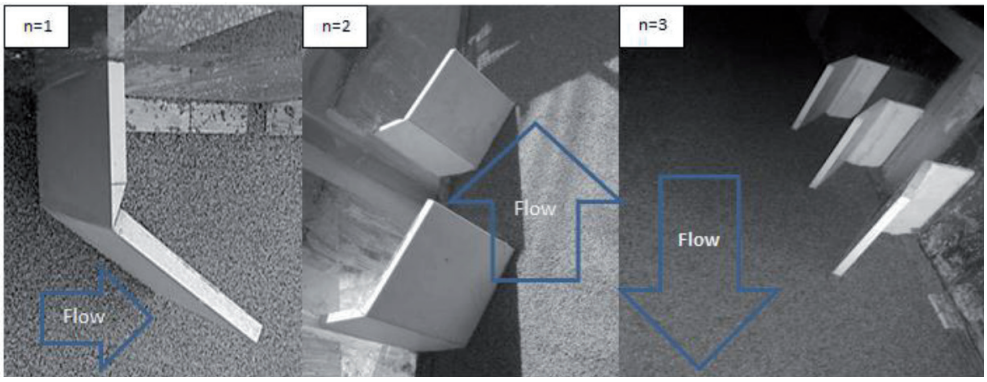

FIGURE 6. Three arrangements for the V-shaped spur-dikes placed in the flume
Source: own work.

Sediment of flume bed

The current work uses the cohesionless uniform sediment as the flume bed. The results of the mechanical sieve analysis should show that this sand had a median particle grains size d_{50} equivalent to 0.7 mm, and since it is not larger than 0.7 mm, there is no rippling formation. The sand size geometric standard deviation (σ_g) was equal to 1.31 to ensure the sediment uniformity that is essential to eliminate the armoring effect, which takes place if the sediment is non-uniform.

The experimental work conditions

The applied conditions for all experiments were clear water flowing in a subcritical steady state on a zero-flume bed. Several experiment sets (56 experiments) were performed, showing the impact of the essential parameters on the whole scouring process and the maximum depth of scour: flow depth (y), flow velocity (v), Froude number (Fr), spur-dikes number (n), and distance between spur-dikes (b).

Alasadi, L. A. R., Khlif, T. H., Hassan, F. A. (2023). Experimental investigation for the local scour around V-shaped spur-dikes. *Sci. Rev. Eng. Env. Sci.*, *32* (1), 69–86. DOI 10.22630/srees.4506

Performed study had some limitations: 400-milimeter width of the flume, 130-milimeter length of the spur-dike, three distances between the spur-dikes (130 mm, 195 mm, 260 mm), three types of tested spur-dikes (single, double, and triple), flow depth ranged from 16 to 46 mm, and lastly flow velocity ranged from 0.151 to 0.222 $m \cdot s^{-1}$.

Each laboratory experiment was performed under specific hydraulic parameters, which were the flow depth and velocity in the flume, as shown in Table 1.

TABLE 1. The studied experimental parameters

Run	Flow depth (y) [mm]	Flow velocity (v) [$m \cdot s^{-1}$]	Critical velocity (v_c) [$m \cdot s^{-1}$]	Distance between spur-dikes (b) [mm]	n	Run	Flow depth (y) [mm]	Flow velocity (v) [$m \cdot s^{-1}$]	Critical velocity (v_c) [$m \cdot s^{-1}$]	Distance between spur-dikes (b) [mm]	n
1	$2.1 \cdot 10^{1}$	$2.22 \cdot 10^{-1}$	$2.436 \cdot 10^{-1}$	–	S	29	$4.6 \cdot 10^{1}$	$1.8 \cdot 10^{-1}$	$2.81 \cdot 10^{-1}$	$1.3 \cdot 10^{2}$	D
2	$2.1 \cdot 10^{1}$	$1.981 \cdot 10^{-1}$	$2.436 \cdot 10^{-1}$	–	S	30	$3.6 \cdot 10^{1}$	$1.8 \cdot 10^{-1}$	$2.7 \cdot 10^{-1}$	$1.3 \cdot 10^{2}$	D
3	$2.1 \cdot 10^{1}$	$1.752 \cdot 10^{-1}$	$2.436 \cdot 10^{-1}$	–	S	31	$2.6 \cdot 10^{1}$	$1.8 \cdot 10^{-1}$	$2.54 \cdot 10^{-1}$	$1.3 \cdot 10^{2}$	D
4	$2.1 \cdot 10^{1}$	$1.514 \cdot 10^{-1}$	$2.436 \cdot 10^{-1}$	–	S	32	$1.6 \cdot 10^{1}$	$1.8 \cdot 10^{-1}$	$2.307 \cdot 10^{-1}$	$1.3 \cdot 10^{2}$	D
5	$4.6 \cdot 10^{1}$	$1.8 \cdot 10^{-1}$	$2.81 \cdot 10^{-1}$	–	S	33	$2.1 \cdot 10^{1}$	$2.22 \cdot 10^{-1}$	$2.436 \cdot 10^{-1}$	$2.6 \cdot 10^{2}$	T
6	$3.6 \cdot 10^{1}$	$1.8 \cdot 10^{-1}$	$2.7 \cdot 10^{-1}$	–	S	34	$2.1 \cdot 10^{1}$	$1.981 \cdot 10^{-1}$	$2.436 \cdot 10^{-1}$	$2.6 \cdot 10^{2}$	T
7	$2.6 \cdot 10^{1}$	$1.8 \cdot 10^{-1}$	$2.54 \cdot 10^{-1}$	–	S	35	$2.1 \cdot 10^{1}$	$1.752 \cdot 10^{-1}$	$2.436 \cdot 10^{-1}$	$2.6 \cdot 10^{2}$	T
8	$1.6 \cdot 10^{1}$	$1.8 \cdot 10^{-1}$	$2.307 \cdot 10^{-1}$	–	S	36	$2.1 \cdot 10^{1}$	$1.514 \cdot 10^{-1}$	$2.436 \cdot 10^{-1}$	$2.6 \cdot 10^{2}$	T
9	$2.1 \cdot 10^{1}$	$2.22 \cdot 10^{-1}$	$2.436 \cdot 10^{-1}$	$2.6 \cdot 10^{2}$	D	37	$4.6 \cdot 10^{1}$	$1.8 \cdot 10^{-1}$	$2.81 \cdot 10^{-1}$	$2.6 \cdot 10^{2}$	T
10	$2.1 \cdot 10^{1}$	$1.981 \cdot 10^{-1}$	$2.436 \cdot 10^{-1}$	$2.6 \cdot 10^{2}$	D	38	$3.6 \cdot 10^{1}$	$1.8 \cdot 10^{-1}$	$2.7 \cdot 10^{-1}$	$2.6 \cdot 10^{2}$	T
11	$2.1 \cdot 10^{1}$	$1.752 \cdot 10^{-1}$	$2.436 \cdot 10^{-1}$	$2.6 \cdot 10^{2}$	D	39	$2.6 \cdot 10^{1}$	$1.8 \cdot 10^{-1}$	$2.54 \cdot 10^{-1}$	$2.6\ 10^{2}$	T
12	$2.1 \cdot 10^{1}$	$1.514 \cdot 10^{-1}$	$2.436 \cdot 10^{-1}$	$2.6 \cdot 10^{2}$	D	40	$1.6 \cdot 10^{1}$	$1.8 \cdot 10^{-1}$	$2.307 \cdot 10^{-1}$	$2.6 \cdot 10^{2}$	T
13	$4.6 \cdot 10^{1}$	$1.8 \cdot 10^{-1}$	$2.81 \cdot 10^{-1}$	$2.6 \cdot 10^{2}$	D	41	$2.1 \cdot 10^{1}$	$2.22 \cdot 10^{-1}$	$2.436 \cdot 10^{-1}$	$1.95 \cdot 10^{2}$	T
14	$3.6 \cdot 10^{1}$	$1.8 \cdot 10^{-1}$	$2.7 \cdot 10^{-1}$	$2.6 \cdot 10^{2}$	D	42	$2.1 \cdot 10^{1}$	$1.981 \cdot 10^{-1}$	$2.436 \cdot 10^{-1}$	$1.95 \cdot 10^{2}$	T
15	$2.6 \cdot 10^{1}$	$1.8 \cdot 10^{-1}$	$2.54 \cdot 10^{-1}$	$2.6 \cdot 10^{2}$	D	43	$2.1 \cdot 10^{1}$	$1.752 \cdot 10^{-1}$	$2.436 \cdot 10^{-1}$	$1.95 \cdot 10^{2}$	T
16	$1.6 \cdot 10^{1}$	$1.8 \cdot 10^{-1}$	$2.307 \cdot 10^{-1}$	$2.6 \cdot 10^{2}$	D	44	$2.1 \cdot 10^{1}$	$1.514 \cdot 10^{-1}$	$2.436 \cdot 10^{-1}$	$1.95 \cdot 10^{2}$	T
17	$2.1 \cdot 10^{1}$	$2.22 \cdot 10^{-1}$	$2.436 \cdot 10^{-1}$	$1.95 \cdot 10^{2}$	D	45	$4.6 \cdot 10^{1}$	$1.8 \cdot 10^{-1}$	$2.81 \cdot 10^{-1}$	$1.95 \cdot 10^{2}$	T
18	$2.1 \cdot 10^{1}$	$1.981 \cdot 10^{-1}$	$2.436 \cdot 10^{-1}$	$1.95 \cdot 10^{2}$	D	46	$3.6 \cdot 10^{1}$	$1.8 \cdot 10^{-1}$	$2.7 \cdot 10^{-1}$	$1.95 \cdot 10^{2}$	T
19	$2.1 \cdot 10^{1}$	$1.752 \cdot 10^{-1}$	$2.436 \cdot 10^{-1}$	$1.95 \cdot 10^{2}$	D	47	$2.6 \cdot 10^{1}$	$1.8 \cdot 10^{-1}$	$2.54 \cdot 10^{-1}$	$1.95 \cdot 10^{2}$	T
20	$2.1 \cdot 10^{1}$	$1.514 \cdot 10^{-1}$	$2.436 \cdot 10^{-1}$	$1.95 \cdot 10^{2}$	D	48	$1.6 \cdot 10^{1}$	$1.8 \cdot 10^{-1}$	$2.307 \cdot 10^{-1}$	$1.95 \cdot 10^{2}$	T
21	$4.6 \cdot 10^{1}$	$1.8 \cdot 10^{-1}$	$2.81 \cdot 10^{-1}$	$1.95 \cdot 10^{2}$	D	49	$2.1 \cdot 10^{1}$	$2.22 \cdot 10^{-1}$	$2.436 \cdot 10^{-1}$	$1.3 \cdot 10^{2}$	T
22	$3.6 \cdot 10^{1}$	$1.8 \cdot 10^{-1}$	$2.7 \cdot 10^{-1}$	$1.95 \cdot 10^{2}$	D	50	$2.1 \cdot 10^{1}$	$1.981 \cdot 10^{-1}$	$2.436 \cdot 10^{-1}$	$1.3 \cdot 10^{2}$	T
23	$2.6 \cdot 10^{1}$	$1.8 \cdot 10^{-1}$	$2.54 \cdot 10^{-1}$	$1.95 \cdot 10^{2}$	D	51	$2.1 \cdot 10^{1}$	$1.752 \cdot 10^{-1}$	$2.436 \cdot 10^{-1}$	$1.3 \cdot 10^{2}$	T
24	$1.6 \cdot 10^{1}$	$1.8 \cdot 10^{-1}$	$2.307 \cdot 10^{-1}$	$1.95 \cdot 10^{2}$	D	52	$2.1 \cdot 10^{1}$	$1.514 \cdot 10^{-1}$	$2.436 \cdot 10^{-1}$	$1.3 \cdot 10^{2}$	T
25	$2.1 \cdot 10^{1}$	$2.22 \cdot 10^{-1}$	$2.436\ 10^{-1}$	$1.3 \cdot 10^{2}$	D	53	$4.6 \cdot 10^{1}$	$1.8 \cdot 10^{-1}$	$2.81 \cdot 10^{-1}$	$1.3 \cdot 10^{2}$	T
26	$2.1 \cdot 10^{1}$	$1.981 \cdot 10^{-1}$	$2.436\ 10^{-1}$	$1.3 \cdot 10^{2}$	D	54	$3.6 \cdot 10^{1}$	$1.8 \cdot 10^{-1}$	$2.7 \cdot 10^{-1}$	$1.3 \cdot 10^{2}$	T
27	$2.1 \cdot 10^{1}$	$1.752 \cdot 10^{-1}$	$2.436 \cdot 10^{-1}$	$1.3 \cdot 10^{2}$	D	55	$2.6 \cdot 10^{1}$	$1.8 \cdot 10^{-1}$	$2.54 \cdot 10^{-1}$	$1.3 \cdot 10^{2}$	T
28	$2.1 \cdot 10^{1}$	$1.514 \cdot 10^{-1}$	$2.436 \cdot 10^{-1}$	$1.3 \cdot 10^{2}$	D	56	$1.6 \cdot 10^{1}$	$1.8 \cdot 10^{-1}$	$2.307 \cdot 10^{-1}$	$1.3 \cdot 10^{2}$	T

S – single spur-dike; D – double spur-dike; T – triple spur-dike.

Source: own work.

It is important to know the time required to obtain the scour equilibrium conditions in all experiments to eliminate the time effect. Therefore, at the beginning, we made four experiments, each with a different flow velocity, where the scour was registered every 15 min by a point gauge to measure the maximum ± scour depth at the upstream nose of the spur-dike. To reach stable conditions, four experiments continued for 360 min until no more scour occurred in case of increasing time. From these four experiments it was observed that almost 95–97% of local scour took place through the first 3.5 h, and for more accuracy, all experiments were done within 4 h to exclude the time effect.

Analysis and discussion of results

Tests were designed to evaluate maximum values. The depth of scouring formed nearby spur-dikes is considered the primary step in designing their foundations. Different configurations are made with V-shaped spur-dikes to examine and study the scour phenomenon.

Flow depth (y). Using a different number of spur-dikes, Figure 7 shows the flow depth influence on scour depth (d_s) where it discerns that increasing flow depth (y)

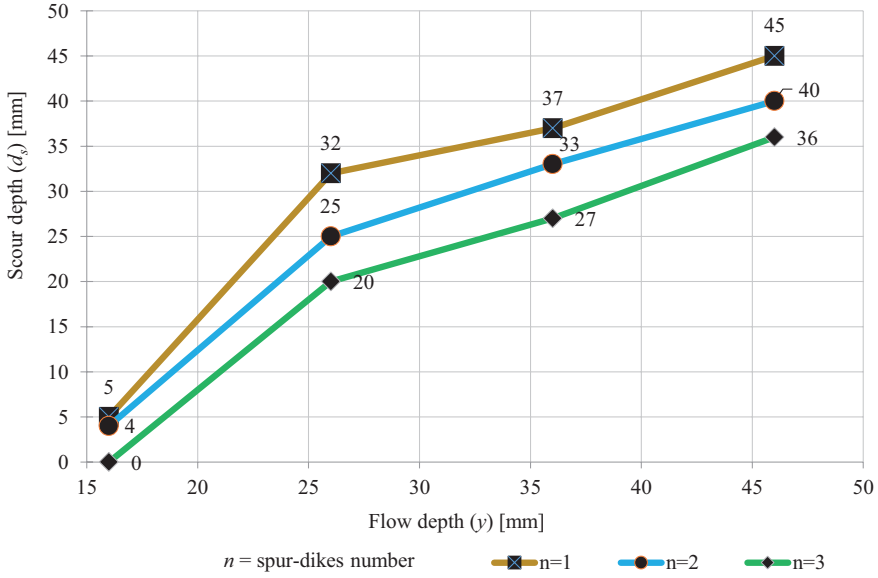

FIGURE 7. Effect of flow depth (y) on scour depth (d_s) development
Source: own work.

Alasadi, L. A. R., Khlif, T. H., Hassan, F. A. (2023). Experimental investigation for the local scour around V-shaped spur-dikes. *Sci. Rev. Eng. Env. Sci.*, *32* (1), 69–86. DOI 10.22630/srees.4506

will increase the propagation of scour, and hence maximum scour depth becomes much deeper, for example, in the case of a single spur-dike (n = 1); then increasing the water depth from 16 to 26 mm will increase the scour depth by almost 80%, increasing the water depth from 26 to 36 mm will increase the scour depth by almost 30%, and increasing the water depth from 36 to 46 mm will increase the scour depth by almost 23%. This scenario occurred while all other influencing parameters were kept constant.

Flow velocity (*V*). In the case of velocity values below the threshold value, the scour depth increases linearly alongside the flow velocity. At the same time, all the remaining parameters are kept steady, as illustrated in Figure 8.

Froude number (*Fr*). Figure 9 depicts the relation between *Fr* and a dimensionless fraction (d_s/y). The plotted figure shows that any increase in *Fr* will increase ds at stable values regarding the remaining factors.

Spur-dikes number (*n*). Figure 10 presents the significant influence of the number of spur-dikes in the decreasing scour process. The other influencing parameters were held constant; the scour depths were reduced when increasing the number of spur-dikes (in the limitation of this study) due to the interference and weakening of the strength of the overlapping horseshoe sort resulting from the sequential

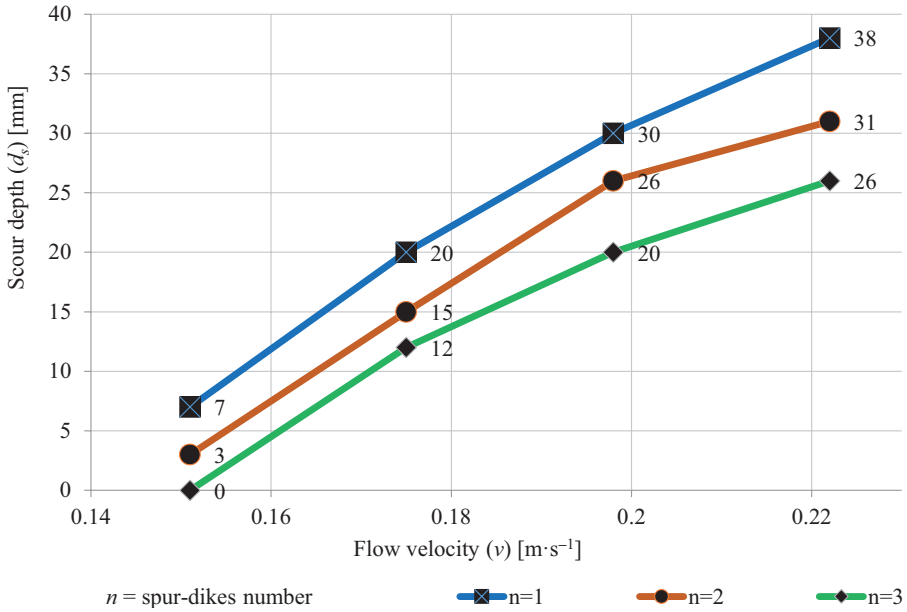

FIGURE 8. Effect of flow velocity (v) change on scour depth (d_s) development
Source: own work.

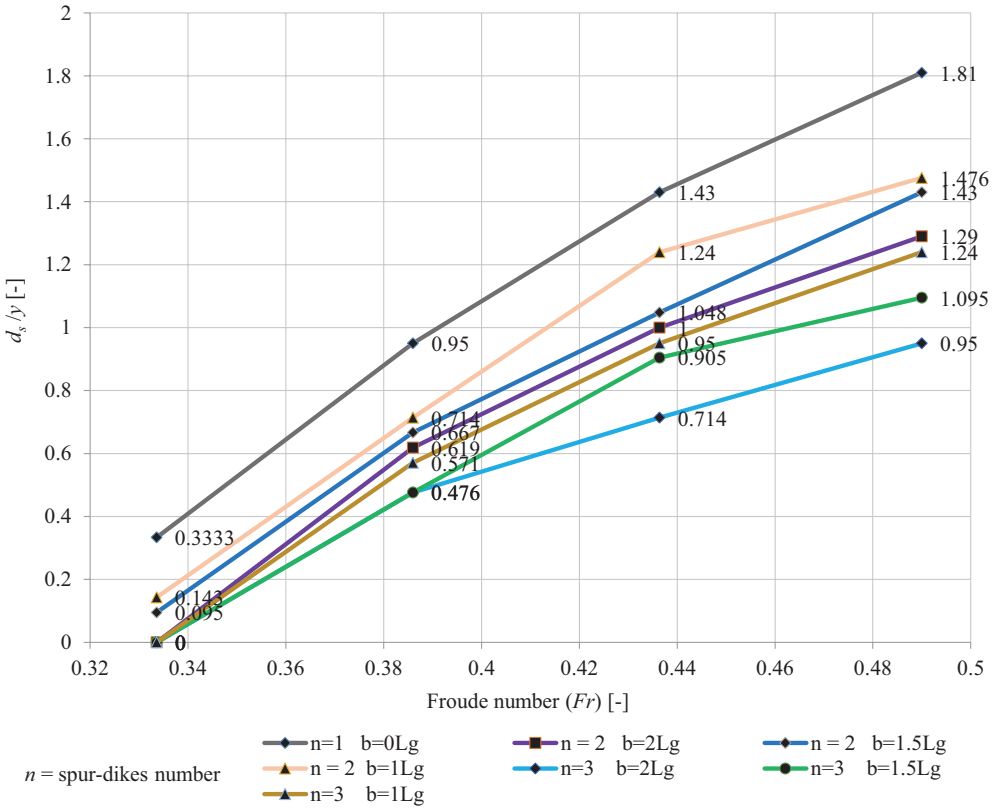

FIGURE 9. Effect of Froude number (*Fr*) change on dimensionless fraction (d_s/y) development
Source: own work.

spur-dikes. It was found that for maximum values of F_r; when an increasing number of spur-dikes changed from single to double; the decreasing percentage in scour depth was about 29%, whereas it was about 26% when the increasing spur-dikes number changed from double to triple.

Distance between spur-dikes (*b*). Three different distances between spur--dikes, and the triple and double spur-dike configurations were utilized to show the distance change effects on the scour depth. Figure 11 shows the estimation for the scour depth to decrease by a percentage ranged from 3.2 to 10% for each $0.5L_g$ increase in the distance between double spur-dikes, while the scour depth decreased by a percentage ranged from about 11.5 to 13% for each $0.5L_g$ increase in the distance between the triple spur-dikes in the limit of the study and in case of fixing all other studied parameters.

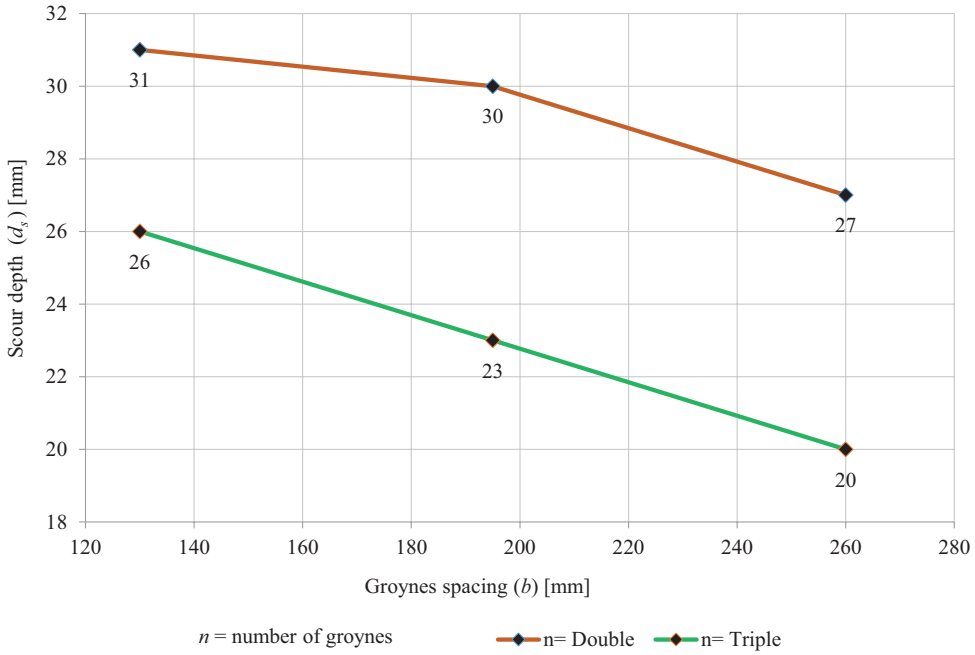

FIGURE 10. Effect of groynes spacing (b) on scour depth (d_s) development
Source: own work.

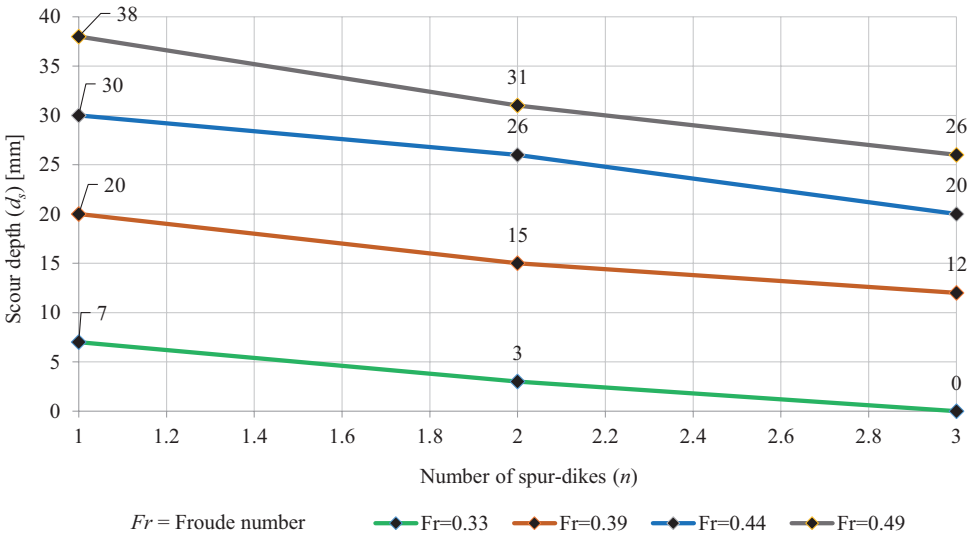

FIGURE 11. Effect of spur-dikes spacing on scour depth (d_s) development
Source: own work.

Comparison with the previous study. The results obtained from this study were compared with a previous study (Al-Yassiry, 2015) that had very similar conditions: the width of the flume in both studies was 40 cm, flow depth ranged from 20 to 21 mm for some studies, flow velocity ranged from 0.222 to 0.23 $m \cdot s^{-1}$ in both studies, with a similar spur-dikes length of 130 mm and similar spur-dikes number. The difference was the shape of spur-dikes to visualize its effect on the maximum scour depth. The results are summarized in Table 2.

TABLE 2. Tests results comparison

n	Distance between spur-dikes (*b*) [mm]	Previous study			Current study
		spur-dikes shape			
		straight	L-head	T-head	V-shape
1	–	58	66	68	38
2	260	55	57	62	27
3	260	55	55	59	20

Source: own work.

Table 2 shows that the V-shaped (checkmark) spur-dikes had the least max values. For the local scour, despite the similar conditions, in fact, the reduction percentage in maximum scour depth was 35–64%, 42–64%, and 44–66% for the straight, L-head, and T-head spur-dikes, respectively, when they compared with the checkmark spur-dikes.

A new formula developing

Utilizing the technique of a dimensional analysis, a dimensionless formula was presented to link the depths of scouring with the studied variables:

$$d_s/y = F(b/y, n, F_r, v/v_c). \tag{4}$$

Then, utilizing the IBM SPSS statistics, the experimental data were analyzed through non-linear regression to produce a formula for calculating the dimensionless fraction (d_s/y) as follows:

$$d_s/y = \left[C_1\left(b/y\right)\right] + \left[C_2\left(Fr^{C_3}\right)\right] + \left[C_4\left(v/v_c^{C_5}\right)\right] + \left(n^{C_6}\right) + C_7, \tag{5}$$

$C_1 = –0.015$, $C_2 = –55.591$, $C_3 = 3.936$, $C_4 = 7.807$, $C_5 = 2.592$, $C_6 = –0.317$, $C_7 = –2.122$.

Alasadi, L. A. R., Khlif, T. H., Hassan, F. A. (2023). Experimental investigation for the local scour around V-shaped spur-dikes. *Sci. Rev. Eng. Env. Sci.*, *32* (1), 69–86. DOI 10.22630/srees.4506

The determination coefficient for Eq. (5) was equal to 0.954. After arrangements and simplifications, the formula changes into:

$$d_s / y = \left[-0.015\left(b / y\right)\right] - \left[55.591\left(Fr^{3.936}\right)\right] + \left[7.807\left(v / v_c^{2.592}\right)\right] + n^{-0.317} - 2.122. \tag{6}$$

To examine Eq. (6) reliability, 20% of the original experimental records were entered into the formula itself, then a comparison between the observed and predicted values of $d_s/_y$ was made. The value of $R^2 = 0.974$ is obtained to reflect the excellent agreement to all records, as shown in Figure 12.

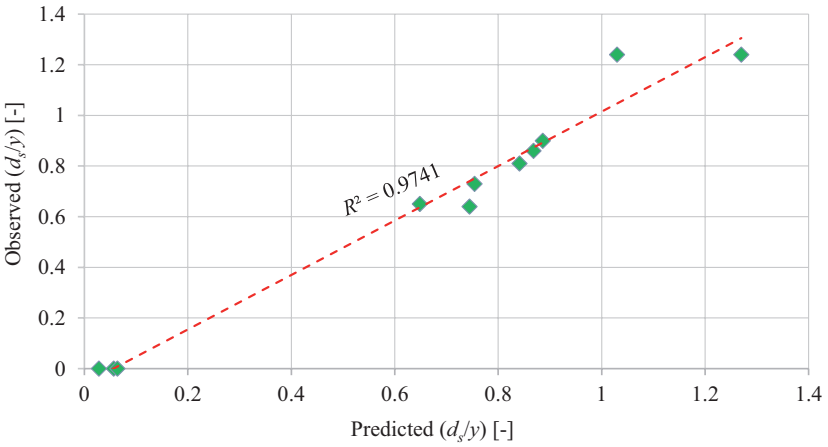

FIGURE 12. Observed and predicted values of dimensionless fraction (d_s/y) comparison
Source: own work.

Conclusions

The following conclusions were observed for the present study:

1. The scour depths changed directly with the Froude number (F_r), mean approach velocity of the flow (v) and flow depth (y). When the distance and number of spur-dikes are constant, the scour depths are increased by the hydraulic conditions. In the case of a single spur-dike ($n = 1$), increasing the water depth from 16 to 26 mm will increase the scour depth by almost 80%, increasing the water depth from 26 to 36 mm will increase the scour depth by almost 30%, and increasing the water depth from 36 to 46 mm will increase the scour depth by almost 23%.

2. In the limitation of this study and for constant flow depth and velocity, the scour depths decreased while increasing the spur-dike number and the distance between them. It was found that for maximum *Fr* values, there was an increasing number of spur-dikes from single to double; the decreasing percentage in scour depth was about 29%, whereas it was about 26% when increasing spur--dikes number from double to triple.
3. The scour depth was estimated to decrease by about 3.2 to 10% for each $0.5L_g$ increase in the distance between double spur-dikes, while the scour depth decreased by about 11.5 to 13% for each $0.5L_g$ increase in the distance between triple spur-dikes in the limit of the study and in case of fixing all the other studied parameters.
4. The deepest scour occurred in the spur-dike nose at the upstream face.
5. The first spur-dike always faces the maximum scour due to its location.
6. The best arrangement for double and triple spur-dikes was when they had a double spur length distance between them. Of course, when the number of spurs is three, it is better because it offers more protection for the river banks.

Data availability statement

Most datasets generated and analyzed in this study are comprised in this submitted manuscript. The other datasets are available on reasonable request from the corresponding author with the attached information.

References

Al Shaikhli, H. I. & Kadhim, K. N. (2018). Development an equations for flow over weirs using MNLR and CFD simulation approaches. *International Journal of Civil Engineering and Technology*, *9* (3), 70–79.

Al-Yassiry, H. H. (2015). *Investigation of local scour around curved groynes* (MSc thesis). Kufa: University of Kufa.

Espandar, R. & Imam, A. (1994). *Erosion control methods in rivers* (technical report). Tehran: Niroo Research Institute.

Ezzeldin, M. M., Saafan, T. A., Rageh, O. S. & Nejm, L. M. (2007). Local scour around spur dykes. In *Eleventh International Water Technology Conference, IWTC11* (pp. 779–795). Sharm El-Sheikh.

Jafari, B. & Masjedi, A. (2015). The effect of slot on scouring around spur dike at 180 degree bend. *Advances in Environmental Biology*, *9* (5), 215–220.

Kadota, A. & Suzuki, K. (2010). Local scour and development of sand wave around T-type and L-type groynes. In S. E. Burns, S. K. Bhatia, C. M. C. Avila & B. E. Hunt (Eds), *Scour and Erosion* (pp. 707–714). Reston: American Society of Civil Engineers.

Khsaf, S. I. (1991). *Experimental investigation of scour and deposition around spur-dikes* (MSc thesis). Baghdad: University of Baghdad.

King, H. W., Brater, E. F., Wei, C. Y. & Lindell, P. E. (1996). *Handbook of hydraulics*. New York: McGraw-Hill.

Kurzke, M., Weitbrecht, V. & Jirka, G. H. (2002). Laboratory concentration measurements for determination of mass exchange between groin fields and main stream. *River Flow*, *1*, 369–376.

Lagasse, P. F. & Richardson, E. V. (2001). ASCE compendium of stream stability and bridge scour papers. *Journal of Hydraulic Engineering*, *127* (7), 531–533.

Möws, R. & Koll, K. (2019). Roughness effect of submerged groyne fields with varying length, groyne distance, and groyne types. *Water*, *11* (6), 1253.

Rashad, B. M. (2021). *An experimental study of local scour around submerged groynes* (MSc thesis). University of Basrah, Basrah.

Rashad, B. M. & Kassaf, S. I. (2020). An investigation of the mechanism of local scour and deposition process around submerged (I-shape) groynes. *Journal of Critical Reviews*, *7* (13), 3204–3219.

Toro-Escobar, C., Voigt Jr, R., Melville, B., Chiew, M. & Parker, G. (1998). Riprap performance at bridge piers under mobile-bed conditions. *Transportation Research Record*, *1647* (1), 27–33.

Appendix

The dimensional analysis in the manuscript was the key to determining the important parameters that affect the maximum scour depth located in the nose of V-shaped spur-dike. The method will be described in detail further.

The maximum depth of scour ($d_{s\max}$) could be inscribed in functional form as (for explanation of the operands see the main text):

$$d_{s\max} = f\{y, v, v_c, L_g, \rho, \rho_s, \mathrm{g}, n, b, d_{50}, \mu, \sigma_g, B, S_\circ\}, \tag{1}$$

$$f_1\{d_{s\max}, y, v, v_c, L_g, \rho, \rho_s, \mathrm{g}, n, b, d_{50}, \mu, \sigma_g, B, S_\circ\} = 0. \tag{1a}$$

Since there are 15 variables ($n = 15$) that contain only three primary units ($m = 3$), 12 will be the number of the dimensionless parameters, which came from $n - \mathrm{m}$; thus:

$$f_2\left(\pi_1, \pi_2, \pi_3, \ldots, \pi_{12}\right) = 0. \tag{1b}$$

Each term has $m + 1 = 3 + 1 = 4$ variables if we assume the common variables v, ρ, and y; so, according to the π-theorem:

$\pi_1 = \rho^{a1}\, v^{b1}\, y^{c1}\, d_{S\max}$, $\pi_2 = \rho^{a2}\, v^{b2}\, y^{c2}\, v_c$, $\pi^3 = \rho^{a3}\, v^{b3}\, y^{c3}\, L_g$,

$\pi_4 = \rho^{a4}\, v^{b4}\, y^{c4}\, \rho_s$, $\pi_5 = \rho^{a5}\, v^{b5}\, y^{c5}\, \mathrm{g}$, $\pi_6 = \rho^{a6}\, v^{b6}\, y^{c6} n$,

$\pi_7 = \rho^{a7}\, v^{b7}\, y^{c7}\, b$, $\pi_8 = \rho^{a8}\, v^{b8}\, y^{c8}\, d_{50}$, $\pi^9 = \rho^{a9}\, v^{b9}\, y^{c9}\, \mu$,

$\pi_{10} = \rho^{a10}\, v^{b10}\, y^{c10}\, \sigma_g$, $\pi_{11} = \rho^{a11}\, v^{b11}\, y^{c11} B$, $\pi_{12} = \rho^{a12}\, v^{b12}\, y^{c12}\, S_\circ$.

Then we take each term and equate the exponents of M, L, and T.

$M^0 L^0 T^0 = (M\, L^{-3})^{a1}\, (LT^{-1})^{b1}\, (L)^{c1}\, L$,

M: $0 = a_1 \rightarrow a_1 = 0$,

L: $0 = 3a1 + b_1 + c_1 \rightarrow b_1 + c_1 = 0$,

T: $0 = -b_1 \rightarrow b_1 = 0$, $c_1 = -1$,

$\therefore\ \pi_1 = \rho^0\, v^0\, y^{-1}\, d_{S\max} \Rightarrow\ \pi_1 = \dfrac{d_{S\max}}{y}$.

In the same way, the other π-terms can be written as:

$$\pi_2 = \frac{v}{v_c}, \pi_3 = \frac{L_g}{y}, \pi_4 = \frac{\rho_s}{\rho}, \pi_5 = Fr, \pi_6 = n, \pi_7 = \frac{b}{y}, \pi_8 = \frac{d_{50}}{y}, \pi_9 = \frac{\mu}{\rho v y}, \pi_{10} = \sigma_g, \pi_{11} = \frac{B}{y}, \pi_1$$

$$\therefore 0 = f_3\left(\frac{d_{S\max}}{y}, \frac{v}{v_c}, \frac{L_g}{y}, \frac{\rho_s}{\rho}, Fr, n, \frac{b}{y}, \frac{d_{50}}{y}, \frac{\mu}{\rho v y}, \sigma_g, \frac{B}{y}, S_\circ\right).$$

Now, the above relationship was made simpler by eliminating constant values terms, also enforcing the assumptions (constant viscosity and relative density, single sediment size), then the functional relation is:

$$f_4\left(\pi_1, \pi_2, \pi_4, \pi_5, \pi_6, \pi_7\right) = 0 \ \text{ or } \ f_4\left(\frac{d_{S\max}}{y}, \frac{v}{v_c}, Fr, n, \frac{b}{y}\right) = 0.$$

In terms of the maximum scour depth:

$$\frac{d_{S\max}}{y} = f_5\left(\frac{v}{v_c}, \frac{L_g}{y}, Fr, n, \frac{b}{y}\right). \tag{2}$$

Alasadi, L. A. R., Khlif, T. H., Hassan, F. A. (2023). Experimental investigation for the local scour around V-shaped spur-dikes. *Sci. Rev. Eng. Env. Sci.*, *32* (1), 69–86. DOI 10.22630/srees.4506

Summary

Experimental investigation for the local scour around V-shaped spur-dikes. Spur-dikes are efficient hydraulic structures that are made for numerous purposes. They have one end on the stream bank and another extending into the current. As a result of the existing spur-dikes in the stream course, the local scour phenomena usually occur around them, leading to several predicaments which have been of great concern to the hydraulic engineers. For the present work, laboratory experiments were carried out to measure the scour depths around several spur-dikes located at different distances for the V-shaped one. The experiments were conducted using physical models installed in a non-curved flume with a bed with uniform cohesion-less sediment of a medium particle size (d_{50} = 0.7 mm). All the models were operated under the subcritical flow of clear-water conditions. The investigations include three spur-dikes (1, 2 and 3) and three distances between them (1, 1.5 and 2 of spur-dike length) as two countermeasures to minimize the local scour depths. The results showed that an increasing number of spur-dikes and the distances between them would decrease the scour depths within the limit of the present study. The experimental data were used to create a new formula of R^2 = 0.954 that reflects a good agreement with the experimentally observed results.